PROCEEDINGS OF SPIE

Thermodynamics and crystal growth of Cd1-x-yMnxZnyTe (x=0.10, 0.20, y=0.15)

Kopach, V., Kopach, O., Shcherbak, L., Fochuk, P., Bolotnikov, A. E., et al.

SPIE.

Thermodynamics and crystal growth of Cd$_{1-x-y}$Mn$_x$Zn$_y$Te (x=0.10, 0.20, y=0.15)

V. Kopach[1], O. Kopach[1], L. Shcherbak[1], P. Fochuk[1], A. E. Bolotnikov[2], R. B. James[3]

[1] – Chernivtsi National University, Ukraine
[2] – Brookhaven National Laboratory, USA
[3] – Savannah River National Laboratory, USA

ABSTRACT

In this work the structural, optical and electrical properties of Cd$_{1-x-y}$Mn$_x$Zn$_y$Te single crystals (x=0.10, 0.20, y=0.15) grown by the vertical Bridgman method were investigated. Based on differential thermal analysis results, it was found that the crystallization rate increases as the crystallization temperature (T$_s$) decreases. It is determined that the volume fraction of solid phase in Cd$_{0.75}$Mn$_{0.10}$Zn$_{0.15}$Te and Cd$_{0.65}$Mn$_{0.20}$Zn$_{0.15}$Te alloys decrease to a minimum in the temperature ranges 1366–1389 K and 1363-1388 K, respectively. The activation energies of melting and crystallization processes for these alloys under different conditions are established. The linear character of the dependence between the preexponential factor (ln$\varphi_{\text{sol.phase,0}}$ and ln$V_{\text{melt., sol. phase,0}}$) and the activation energy of these processes is determined, which is evidence of a compensation effect. The band-gap value was estimated to be ~ 1.73 eV for Cd$_{0.75}$Mn$_{0.10}$Zn$_{0.15}$Te and ~1.84 eV for Cd$_{0.65}$Mn$_{0.20}$Zn$_{0.15}$Te at 300 K. Typical transmission images showed the presence of small Te inclusions (5-10 µm) in the crystals. The electrical resistivity, obtained from the I-V curves, was ~10^4 Ω·cm for both crystals and decreased slightly toward the end of the ingots.

Keywords: CMZT, melting/ crystallization processes, band-gap, activation energy and compensation effect, single crystal growth.

1. INTRODUCTION

The thermodynamics of melting and crystallization processes of solid compounds containing volatile components is one of the most important factors for carrying out crystal growth operations. The state of the crystal defect structure almost completely depends on the crystallization temperature. As a result, both the nucleation conditions and the rate of crystal growth essentially affect the quality of the as-grown crystals. In addition, the thermodynamics of melting and crystallization are also applied to obtain a phase diagram, understand deviation of the compound's stoichiometry, and explain the defect structure concentration. [1]

One interesting tool of the thermodynamics is a phenomenon of linear correlations between the logarithms of the pre-exponential factor (lnA_0) and the activation energy (ΔE_a) for different processes described by an Arrhenius equation. Such correlation is known as the compensation effect (CEF) governed by the Meyer-Neldel rule (MNR) [2, 3]. This phenomenon has already been investigated for diffusion [4] and melting/crystallization processes [5, 6] in pure CdTe and CdTe-based ternary solid solutions. In the present work we investigate CEF in more complex CdTe-based solid solutions, namely Cd$_{1-x-y}$Mn$_x$Zn$_y$Te.

The great interest in the quaternary semiconductors Cd$_{1-x-y}$Mn$_x$Zn$_y$Te arises out of the additional control of the growth and material parameters, such as controlling the band-gap value while fixing the lattice constant. In contrast to the ternary Cd$_{1-x}$Mn$_x$Te compound, where the band-gap increases with increasing Mn concentration [7, 8], in the Cd$_{1-x-y}$Mn$_x$Zn$_y$Te system, it is possible to change the concentrations of Zn and Mn without changing the band-gap value [9].

2. EXPERIMENT

Synthesis of Cd$_{1-x-y}$Mn$_x$Zn$_y$Te (x=0.10, 0.20, y=0.15) compounds were carried out with high-purity elements of Te (6N), Cd (6N), Zn (6N) and Mn (4N). The DTA of these alloys was performed with heating/cooling rates equal to 5 and 10 K/min with an intermediate melt dwell time of 30 min. Using the Differential Thermal Analysis (DTA) method, we determined the temperatures of the solid-liquid phase transition of Cd$_{1-x-y}$Mn$_x$Zn$_y$Te alloys and the melting/solidification rates.

Cd$_{1-x-y}$Mn$_x$Zn$_y$Te (x=0.10, 0.20, y=0.15) single-crystal ingots were grown by the vertical Bridgman method. The crystalline nature of the samples was verified by powder XRD patterns using a DRON-3M X-Ray generator. To study

the resistivity, the current-voltage dependencies (I-V curves) were measured using a Keithley 617 electrometer. The optical analysis was performed by the transmission method using an Ocean Optics OO-2000 Spectrometer in the range of 500 – 900 nm.

3. RESULTS AND DISCUSSIONS

3.1. DTA investigation of the $Cd_{1-x-y}Mn_xZn_yTe$ melting-crystallization

To establish the phase equilibrium of the melting/crystallization processes of $Cd_{1-x-y}Mn_xZn_yTe$ (x=0.10, 0.20, y=0.15) alloys, we investigated the dependencies of the crystallization effect's area on the holding temperature. From fig. 1 we can see that below 1391 K (Fig.1, a) and 1396 K (Fig. 1, b), there are no full crystallization process (left Y-axis,
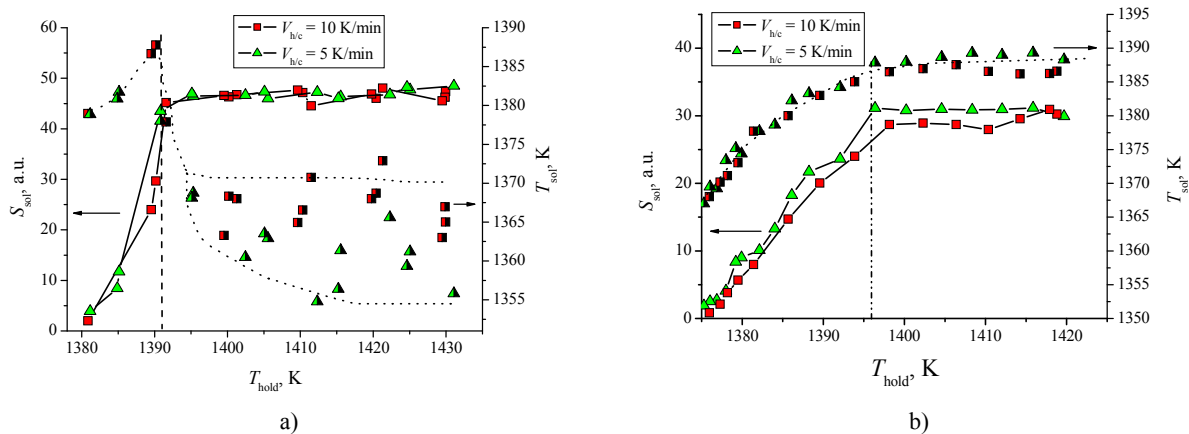

Figure 1. Crystallization effect's area (left scale) and crystallization temperatures (right scale) dependencies on the melt's holding temperature for the $Cd_{0.75}Mn_{0.10}Zn_{0.15}Te$ (a) and $Cd_{0.65}Mn_{0.20}Zn_{0.15}Te$ (b) alloys.

S_{sol} = 10-40 relative units). It means that the holding temperatures are not high enough. Only after increasing the holding temperatures higher then 1391 K (Fig.1, a) and 1396 K (Fig. 1, b), the value of the crystallization effect's area was set at about 50-60 relative units. That is, there is crystallization of the completely melted samples.

Other curves in fig. 1 describe the solidification temperature's dependency on the holding temperatures for the melts $Cd_{0.75}Mn_{0.10}Zn_{0.15}Te$ and $Cd_{0.65}Mn_{0.20}Zn_{0.15}Te$ (right Y-axis). As we can see $Cd_{0.75}Mn_{0.10}Zn_{0.15}Te$ and $Cd_{0.65}Mn_{0.20}Zn_{0.15}Te$ melts are in a semi-liquid state for the holding temperature ranges 1379 – 1391 K and 1376 – 1396 K, respectively - that is, the solid phase is in equilibrium with the liquid. It is obvious that in this case the crystallization of the melts occurs immediately after the cooling process starts. At the same time the melt's crystallization temperatures are higher than the temperature at which the sample begins to melt. Therefore, for destroying all solid phases remaining in the melts, the alloys must be overheated to at least 1391 K and 1395 K for $Cd_{0.75}Mn_{0.10}Zn_{0.15}Te$ and $Cd_{0.65}Mn_{0.20}Zn_{0.15}Te$, respectively.

Figure 2 presents a semi-logarithmic interpretation of the crystallization rates of the Cd0.65Mn0.20Zn0.15Te melt dependences on their crystallization temperature. As can be seen from this figure for both heating/cooling rates, these dependencies are described by Arrhenius equations Vsol = Vsol,0•exp(-Ea/RT), and the melt crystallization process is characterized by Ea in the range of 600-820 kJ/mol.

Comparing the values of E_a with the same data obtained in our earlier manuscript [10] for crystallization process of $Cd_{0.65}Mn_{0.30}Zn_{0.05}Te$ melt (the same content of CdTe in the alloy), we observe the same magnitude of activation energy values. This means that the dominant role in crystallization processes of these alloys belongs to the structure centered on the role of CdTe bonds.

Fig. 3 illustrates the patterns of melting processes for the $Cd_{0.75}Mn_{0.10}Zn_{0.15}Te$ and $Cd_{0.65}Mn_{0.20}Zn_{0.15}Te$ alloys. We can see that the melting temperature of the solid phase does not depend on the holding temperature in the temperature range of 1356-1366 K for $Cd_{0.75}Mn_{0.10}Zn_{0.15}Te$ and 1355-1363 K for $Cd_{0.65}Mn_{0.20}Zn_{0.15}Te$, respectively. An increase of the holding temperature from 1366 K to 1389 K and from 1363 K to 1388 K for $Cd_{0.75}Mn_{0.10}Zn_{0.15}Te$ and $Cd_{0.65}Mn_{0.20}Zn_{0.15}Te$ melts, respectively, leads to an increase of the melting temperature of the solid-phase component remaining in the melts. In this case the samples are in a semi-liquid state with certain composition of a solid phase, which is different from the composition of the original alloy. The rise of the sample's holding temperature above 1389 K for $Cd_{0.75}Mn_{0.10}Zn_{0.15}Te$ and 1388 K for $Cd_{0.65}Mn_{0.20}Zn_{0.15}Te$ does not lead to the registration of melting effect of the
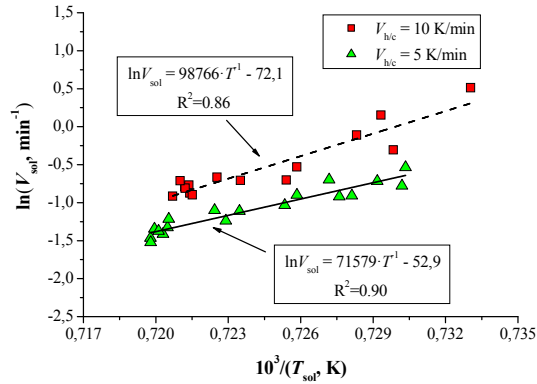
Figure 2. Crystallization rate logarithm versus reciprocal crystallization temperatures for the $Cd_{0.65}Mn_{0.20}Zn_{0.15}Te$ alloys.

solid phase, and therefore we can talk about the homogeneity of the melts under these conditions. Since zinc telluride has the highest melting point in comparison with other (CdTe and MnTe) binary compounds, it is obvious that the solid phase in the melt is enriched with ZnTe in comparison with the composition of the initial alloy. So, its composition depends on the holding temperature of the melt.
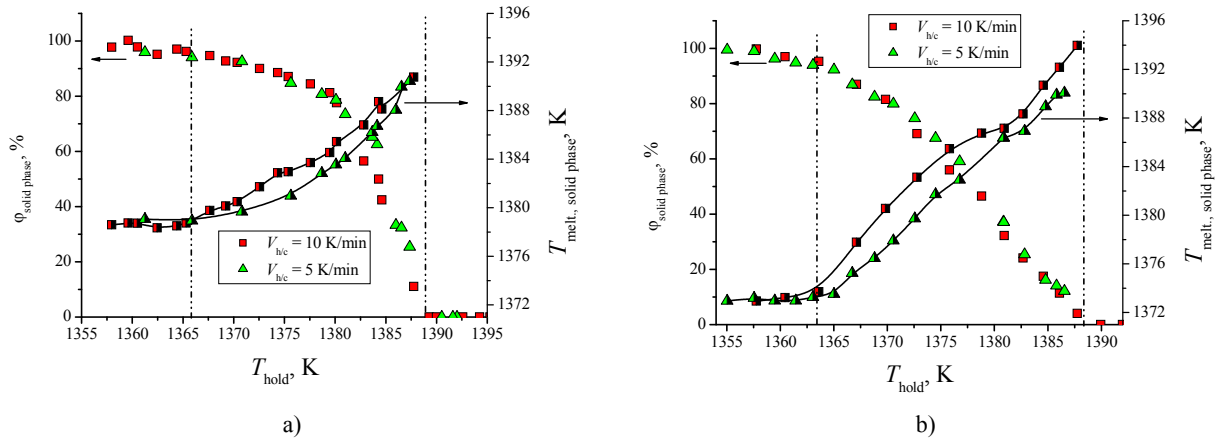

a)   b)

Figure 3. The temperature dependencies of the volume fraction of the solid phase remaining in $Cd_{0.75}Mn_{0.10}Zn_{0.15}Te$ (a) and $Cd_{0.65}Mn_{0.20}Zn_{0.15}Te$ (b) melts.

If we present the above temperature dependencies of the solid phase fraction (Fig. 3) in semi-logarithmic coordinates, the melting of the solid phase is seen as characterized by two different mechanisms (Fig. 4). At
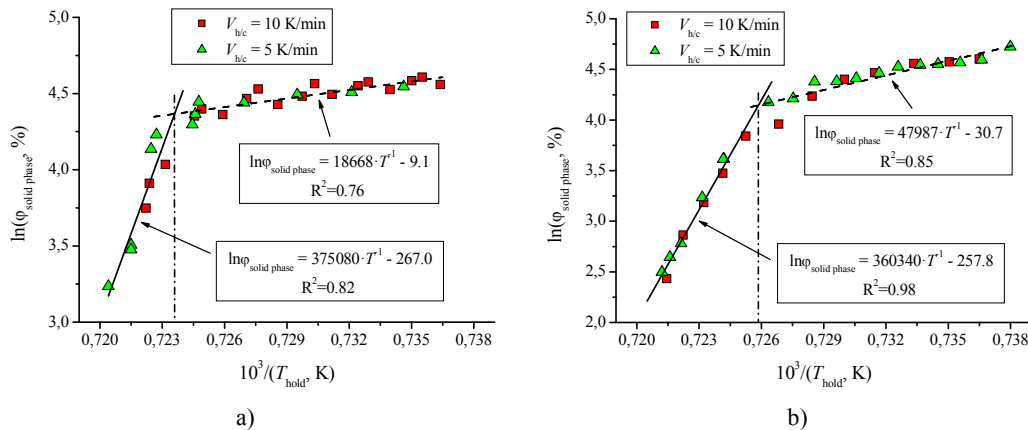

a)   b)

Figure 4. The solid phase (clusters) volume fraction logarithm versus reciprocal holding temperatures for the $Cd_{0.75}Mn_{0.10}Zn_{0.15}Te$ and $Cd_{0.65}Mn_{0.20}Zn_{0.15}Te$ melts.

the temperature 1382 K for the $Cd_{0.75}Mn_{0.10}Zn_{0.15}Te$ alloy and the temperature 1378 K for the $Cd_{0.65}Mn_{0.20}Zn_{0.15}Te$ alloy, the melting of the solid phase occurs with a lower activation energy (155 kJ/mole for $Cd_{0.75}Mn_{0.10}Zn_{0.15}Te$ and 399 kJ/mole for $Cd_{0.65}Mn_{0.20}Zn_{0.15}Te$), and it is obvious that at this stage there is a break of bonds with less energy. When the solid phase is heated above these critical temperatures, the mechanism of the solid phase fragmentation (clusters) changes to the clusters dissolving from the surface, obviously, and this process requires more energy (3118 kJ/mole for $Cd_{0.75}Mn_{0.10}Zn_{0.15}Te$ and 2996 kJ/mole for $Cd_{0.65}Mn_{0.20}Zn_{0.15}Te$). This is due to the fact that the fragments of the solid phase (clusters) contain a larger content of high-melting components and, possibly, have a different structure. Such transformations are also characteristic for pure and slightly doped CdTe [11]. The results mentioned above at the critical temperatures (1378 K and 1382 K) are also observed for pure CdTe [12]. That fact, that dissolution of $Cd_{0.75}Mn_{0.10}Zn_{0.15}Te$ solid phase which contains more CdTe than $Cd_{0.65}Mn_{0.20}Zn_{0.15}Te$ requires more energy, proofs that the structure of the fragments of the solid phase (clusters) can play important role in the mechanism of their dissociation.

Fig. 5 shows the melting rates logarithm of the remaining solid phases dependences on the reciprocal melting temperature of this phase in the $Cd_{0.75}Mn_{0.10}Zn_{0.15}Te$ and $Cd_{0.65}Mn_{0.20}Zn_{0.15}Te$ melts (after intermediate holdings). Figure 5 illustrates that in both cases the melting of the solid phase occurs faster in the case of higher heating rate (10 K/min), and this process occurs with less activation energy (719 kJ/mole ($V_{h/c}$ = 10 K/min) vs. 749 kJ/mole ($V_{h/c}$ = 5 K/min) for $Cd_{0.75}Mn_{0.10}Zn_{0.15}Te$ and 870 kJ/mole ($V_{h/c}$ = 10 K/min) vs. 1222 kJ/mole ($V_{h/c}$ = 5 K/min) for $Cd_{0.65}Mn_{0.20}Zn_{0.15}Te$). In addition, the melting of the $Cd_{0.65}Mn_{0.20}Zn_{0.15}Te$ alloy, which has a larger content of MnTe occurs with higher activation energies, which, obviously, may be associated with a higher energy of the Mn-Te bond compared to the energy of the Cd-Te bond.
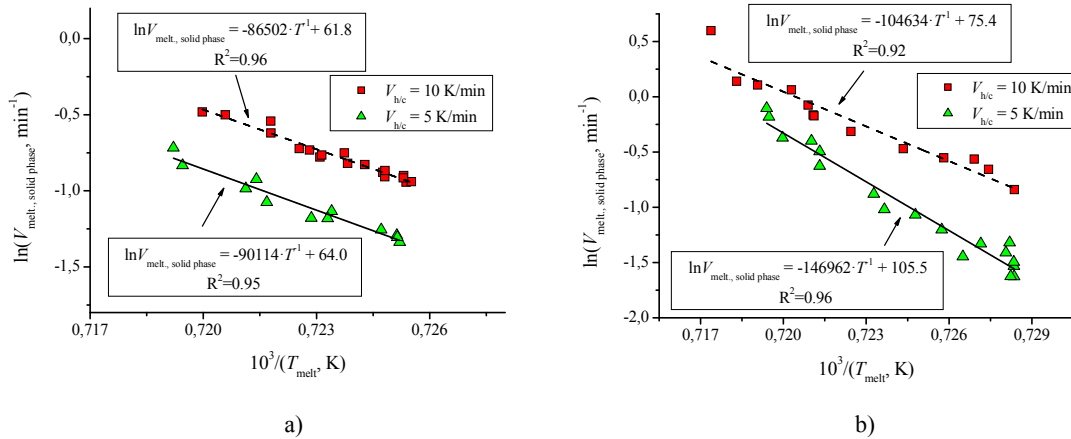

a)   b)

Figure 5. Solid phase melting rate versus reciprocal melting temperatures for the $Cd_{0.75}Mn_{0.10}Zn_{0.15}Te$ (a) and $Cd_{0.65}Mn_{0.20}Zn_{0.15}Te$ (b) alloys.

According to the lines positions in Fig. 4, the temperature dependence of the volume fraction of the solid phase (clusters) for each alloy is described by the Arrhenius-type equation (Eq. 1) in two temperature intervals.

$$\varphi_{sol.\ phase} = \varphi_{sol.phase,0} \cdot \exp(-E_a/RT) \qquad (1)$$

Fig. 5 states the same for the temperature dependences of the melting rate of the solid phase in the melt (Eq. 2).

$$V_{melt.,\ sol.\ phase} = V_{melt.,\ sol.\ phase,0} \cdot \exp(-E_a/RT) \qquad (2)$$

If we extract corresponding numerical values from the equations shown in Fig. 4 ($\ln\varphi_{sol.phase,0}$ and E_a) and Fig. 5 ($\ln V_{melt.,\ sol.\ phase,0}$ and E_a), and build the dependence of the logarithm of the preexponential factor on the activation energy, we see that these values are described by a linear dependence (Fig. 6) proving the compensation effect. It should be noted that to compare the data in Fig. 4 with the data in Fig. 5 for the latter we used the inverse values, because the lines have different slopes. In addition, in Fig. 6 we plotted the same data from [5] for melting parameters of pure CdTe and weakly doped by In, Ge, Sn. All the data visualize the clear relationship between the thermodynamic parameters of melting process of the solid phase based on CdTe. Fig. 6 illustrates that the values of the activation energy of the solid phase dissolution process in temperature interval in which temperatures are less then the critical temperature (T < 1382 K for the $Cd_{0.75}Mn_{0.10}Zn_{0.15}Te$ alloy (Fig. 4, a) and T < 1378 K for the $Cd_{0.65}Mn_{0.20}Zn_{0.15}Te$ alloy (Fig. 4, b). Compared with data from [5], they are close to values for the CdTe + 2 mol. % In alloy (see insert in fig. 6). This may be due to the fact that the $Cd_{0.75}Mn_{0.10}Zn_{0.15}Te$ and $Cd_{0.65}Mn_{0.20}Zn_{0.15}Te$ alloys are solid solutions, and indium with CdTe also forms ideal
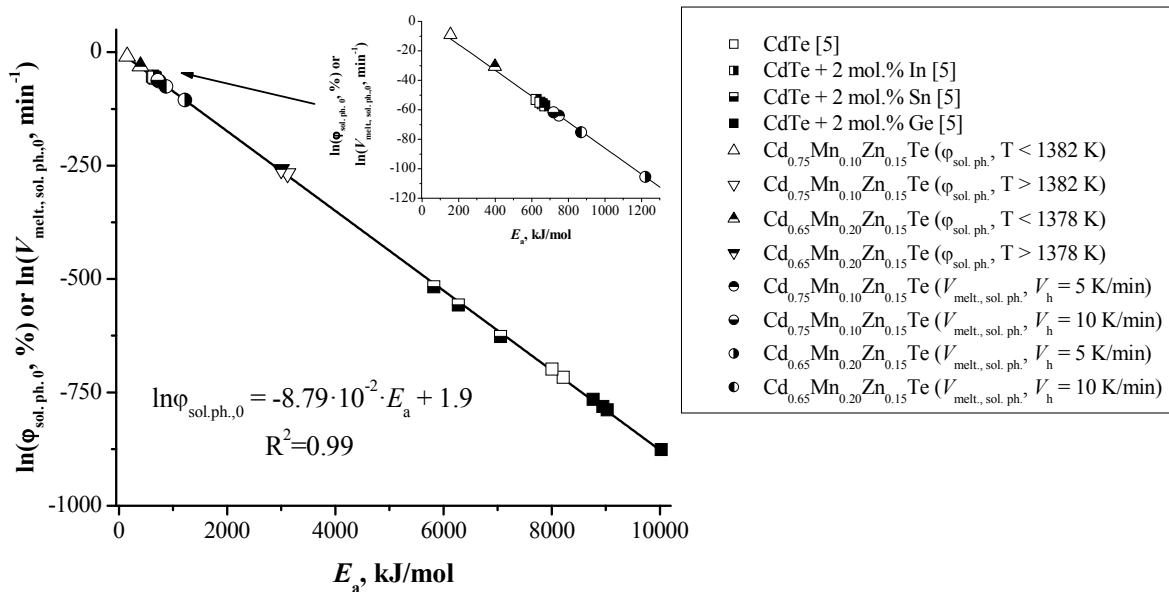
Figure 6. Correlation between equations' parameters of temperature dependencies of the solid-phase volume fraction (or melting rate) in CdTe-based melts (pre-exponential factor and activation energy of the alloys melting process).

solid solutions [13]. If we compare the values of the activation energy of the solid phase dissolution process in high-temperature intervals (T > 1382 K for the $Cd_{0.75}Mn_{0.10}Zn_{0.15}Te$ alloy (Fig. 4, a) and T > 1378 K for the $Cd_{0.65}Mn_{0.20}Zn_{0.15}Te$ alloy (Fig. 4, b), where the fragments of the solid phase have a polygenic structure, these values are shifted towards values for pure CdTe and CdTe + 2 mol.% Ge (Sn). The reason for this may be the presence of clusters of different structure - tetrahedral fragments, hexagonal rings, etc., the presence of which is assumed in melts based on CdTe in [11, 12].

3.2. $Cd_{1-x-y}Mn_xZn_yTe$ crystals growth and characterizations

Using the data obtained from the DTA experiments for $Cd_{0.75}Mn_{0.10}Zn_{0.15}Te$ and $Cd_{0.65}Mn_{0.20}Zn_{0.15}Te$ melts, the ingots with these compositions were grown by the vertical Bridgman method (Fig. 7). We cut the grown ingots into wafers and observed a large number of blocks, in particular at the beginning of grown crystals. We obtained polycrystalline ingots because, presumably, it was several crystallization centers during growth process. In the direction of growth, the numbers of blocks in the ingots decreased. These results can be explained by a different degree of melt axial superheating. The crystals were grown at a temperature gradient. The top of the ampoule was overheated to a high temperature, while the bottom of the ampoule had a slightly lower temperature. The most superheated part of the melt is the upper part (~ 1420 ± 2 K for both alloys) and least superheated is the lower part (~ 1392 ± 2 K for both alloys). Therefore, the lower part was minimal melt superheating above the critical temperature 1391 K for $Cd_{0.75}Mn_{0.10}Zn_{0.15}Te$ alloy (Fig. 1, a) and slightly less then critical temperature 1396 K for $Cd_{0.65}Mn_{0.20}Zn_{0.15}Te$ alloy (Fig. 1, b), that is the $Cd_{0.65}Mn_{0.20}Zn_{0.15}Te$ melt contained much of nuclei which act as crystallization centers. As a result, at the lower part for $Cd_{0.75}Mn_{0.10}Zn_{0.15}Te$ ingot, there are a smaller number of blocks (Fig. 7, a) but much more for the $Cd_{0.65}Mn_{0.20}Zn_{0.15}Te$ ingot (Fig. 7, b).

IR-images in the Fig. 7 (right columns) show the presence of small inclusions (ø 5-10 μm) in the volume of the $Cd_{0.75}Mn_{0.10}Zn_{0.15}Te$ and $Cd_{0.65}Mn_{0.20}Zn_{0.15}Te$ crystals. The number of inclusions in the middle part of both ingots (g = 0.5) is greater than in their upper parts, and they are distributed evenly over the entire plane of both crystals. Only in the upper part of the $Cd_{0.75}Mn_{0.10}Zn_{0.15}Te$ ingot, we can observe large inclusions (more than ø 10 μm), which are somewhat randomly distributed.
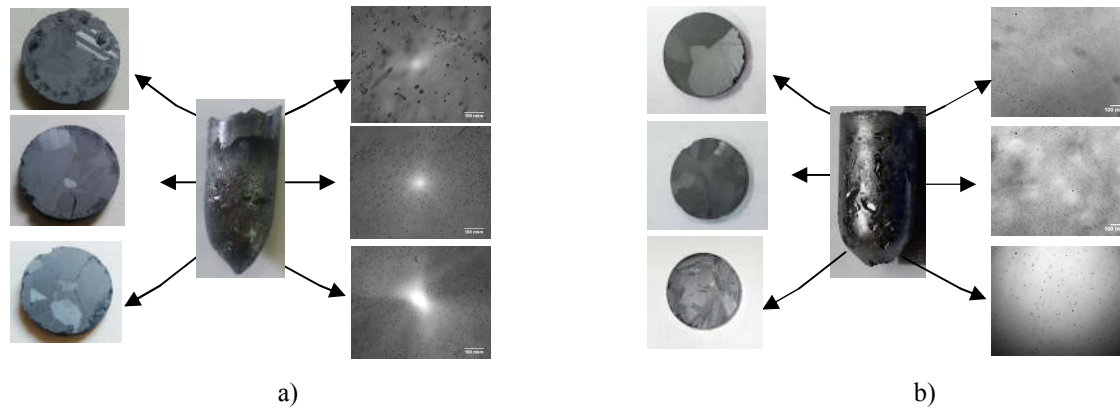
Figure 7. Photo of as-grown $Cd_{0.75}Mn_{0.10}Zn_{0.15}Te$ (a) and $Cd_{0.65}Mn_{0.20}Zn_{0.15}Te$ (b) crystals.

Fig. 8a shows X–ray diffraction patterns of the $Cd_{0.75}Mn_{0.10}Zn_{0.15}Te$ and $Cd_{0.65}Mn_{0.20}Zn_{0.15}Te$ crystals. From the structural analysis we determined the lattice parameters for both semiconductors. The lattice constant values are 6,392(8) Å and 6,375(4) Å for $Cd_{0.75}Mn_{0.10}Zn_{0.15}Te$ and $Cd_{0.65}Mn_{0.20}Zn_{0.15}Te$ crystals respectively. As we can see the lattice constant decreases with increasing MnTe concentration. The reason of this decrease is the smaller covalent atomic radius of Mn (1.326 Å) than of Cd (1.405 Å). Fig. 8b illustrates a comparison of XRD data for as-grown crystal $Cd_{0.65}Mn_{0.20}Zn_{0.15}Te$ (g = 0.5) with XRD peaks of $Cd_{0.50}Mn_{0.35}Zn_{0.15}Te$ [14].
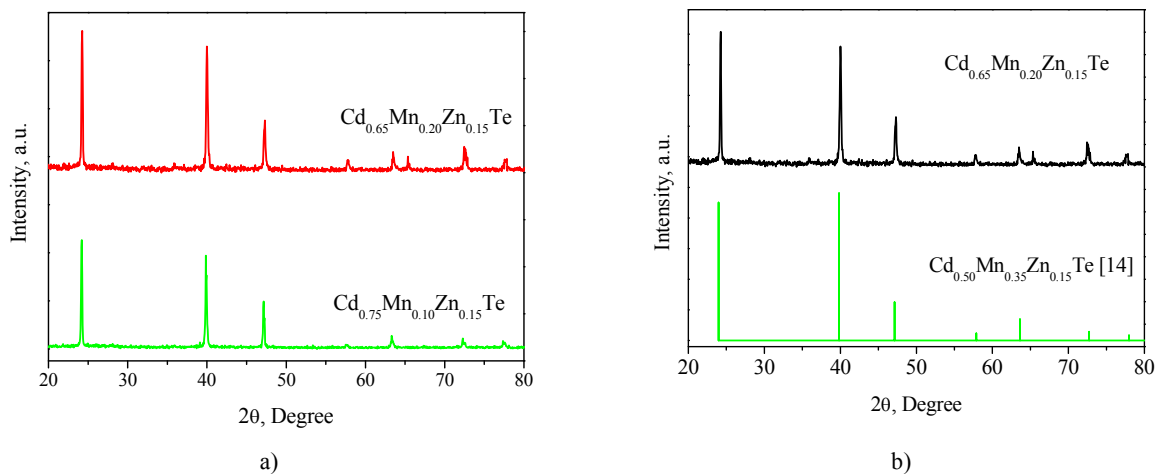
Figure 8. XRD pattern of as-grown $Cd_{0.75}Mn_{0.10}Zn_{0.15}Te$ and $Cd_{0.65}Mn_{0.20}Zn_{0.15}Te$ (a) crystals and XRD pattern of $Cd_{0.65}Mn_{0.20}Zn_{0.15}Te$ (g = 0.5) compared with $Cd_{0.50}Mn_{0.35}Zn_{0.15}Te$ [14] (b).

The band-gap of the grown semiconductor crystals are ~ 1.73 eV and 1.84 eV for $Cd_{0.75}Mn_{0.10}Zn_{0.15}Te$ and $Cd_{0.65}Mn_{0.20}Zn_{0.15}Te$, respectively. These values indicated that with MnTe concentration increasing from 10% to 20 % increased the band-gap value by 0.011 eV per 1% of MnTe. The increase of ZnTe concentration from 10% to 15 % changed the band-gap value of CMZT crystals from 1.67 eV [15] to 1.73 eV for $Cd_{0.90-y}Mn_{0.10}Zn_yTe$ and from 1.78 eV [15] to 1.84 eV for $Cd_{0.80-y}Mn_{0.20}Zn_yTe$ (0.012 eV per 1% ZnTe). Thus, even a slight increasing of MnTe and ZnTe concentration led to increasing of the band-gap value.

The electrical properties of the obtained crystal were established by studying their current-voltage characteristics. From the obtained results the resistance was determined, and the resistivity of the samples was calculated. Both crystals have similar values for the electrical resistivity – $3 \cdot 10^4$ Ohm·cm and $2 \cdot 10^4$ Ohm·cm for $Cd_{0.75}Mn_{0.10}Zn_{0.15}Te$ and $Cd_{0.65}Mn_{0.20}Zn_{0.15}Te$ crystals, respectively.

4. SUMMARY AND CONCLUSIONS

So, we conclude that the dissolution of $Cd_{0.75}Mn_{0.10}Zn_{0.15}Te$ solid phase, which contains more CdTe than $Cd_{0.65}Mn_{0.20}Zn_{0.15}Te$, requires more energy, proof that the structure of the fragments of the solid phase (clusters) in the melt can play an important role in the mechanism of their dissociation. It is also important to note that the melting of the $Cd_{0.65}Mn_{0.20}Zn_{0.15}Te$ alloy, which has a larger content of MnTe, occurs with higher activation energies, which, obviously, may be associated with a higher energy of the Mn-Te bond compared to energy of Cd-Te bond. The dependence of the logarithm of the preexponential factor on the activation energy of melting process for both $Cd_{0.75}Mn_{0.10}Zn_{0.15}Te$ and $Cd_{0.65}Mn_{0.20}Zn_{0.15}Te$ has a linear behavior and corresponds to the compensation effect. These results are in good agreement with previously published results concerning melting and crystallization processes for CdTe-based melts.

Based on the obtained differential thermal analysis data, we grew $Cd_{0.75}Mn_{0.10}Zn_{0.15}Te$ and $Cd_{0.65}Mn_{0.20}Zn_{0.15}Te$ crystals from the melts. According to XRD-analyses the value of the lattice constant of the $Cd_{0.75}Mn_{0.10}Zn_{0.15}Te$ and $Cd_{0.65}Mn_{0.20}Zn_{0.15}Te$ crystals decreases with increasing MnTe concentration. By measuring the transmission spectra, we determined that the band-gap of the grown semiconductor crystals are ~ 1.73 eV for $Cd_{0.75}Mn_{0.10}Zn_{0.15}Te$ and 1.84 eV for $Cd_{0.65}Mn_{0.20}Zn_{0.15}Te$. Both the $Cd_{0.75}Mn_{0.10}Zn_{0.15}Te$ and $Cd_{0.65}Mn_{0.20}Zn_{0.15}Te$ crystals have the same order of electrical resistivity – ~10^4 Ohm·cm.

REFERENCES

1. Nishinaga, T., "Thermodynamics for understanding crystal growth," Progress in Crystal Growth and Characterization of Materials 62 (2), 43-57 (2016).
2. Starikov, E. B. and Norden, B., "Entropy–enthalpy compensation as a fundamental concept and analysis tool for systematical experimental data," Chemical Physics Letters 538, 118-120 (2012).
3. Starikov, E. B., "'Meyer-Neldel Rule': True history of the Development and its Intimate Connection to the Classical Thermodynamics," J. Appl. Sol. Model. 3, 15-31 (2014).
4. Shcherbak, L., Kopach, O., Fochuk, P., Bolotnikov, A. E., and James, R. B., "Empirical Correlations Between the Arrhenius' Parameters of Impurities' Diffusion Coefficients in CdTe Crystals," J. Phase Equilib. Diffus. 36(2), 99-109 (2015).
5. Shcherbak, L., Kopach, O., Fochuk, P., "Solid-liquid Cd(Zn)Te phase transition correlative analysis," J. Cryst. Growth 320, 6–8 (2011).
6. Shcherbak, L. P., Kopach, O. V., "Correlation between Arrhenius equation parameters concerning to Cd(Zn)Te melting and crystallization process," Functional Materials 17 (4), 425-428 (2010).
7. Hwang, Y. and Um, Y., "Magneto-Optical Properties of CdMnTe Single Crystals," Proc. IEEE 978-1-4673-1773 (2013).
8. Kim, K. H., Bolotnikov, A. E., Camarda, G. S., Yang, G., Hossain, A., Cui, Y., James, R. B., Hong, J. and Kim, S. U., "Energy-gap dependence on the Mn mole fraction and temperature in CdMnTe crystal," Journal of Applied Physics 106, 023706-1-3 (2009).
9. Hwang, Y., Chung, S. and Um, Y., "Weak ferromagnetism in CdMnZnTe single crystal," Phys. Stat. Sol. (c) 4 (12), 4457–4460 (2007).
10. Kopach, V., Kopach, O., Fochuk, P., Filonenko, S., Shcherbak, L., Bolotnikov, A. E. and James, R. B., "Vertical Bridgman growth and characterization of $Cd_{0.95-x}Mn_xZn_{0.05}Te$ (x=0.20, 0.30) single-crystal ingots," Proc. SPIE 10392, 1039214-1-8 (2017).
11. Shcherbak, L., Feychuk, P., Kopach, O., Panchuk, O., Hayer, E., Ipser, H., "Fine structure of the melting process in pure CdTe and in CdTe with 2 mol % of Ge or Sn," J. Alloys Comp. 349, 145-151 (2003).
12. Shcherbak, L., "Pre–transition phenomena in CdTe near the melting point," J. Cryst. Growth 197, 397–405 (1999).
13. Tai H., Hori S. "Equilibrium phase diagram for the CdTe–In system," J. Soc. Mater. Sci. (In Japanese) 31, 345–347 (1982).
14. Hwang, Y., Kim, H., Cho, S., Um, Y., Park, H., Jeen, G., "Temperature dependence of the Faraday rotation in diluted magnetic semiconductors $Cd_{1-x-y}Mn_xZn_yTe$ crystals," Journal of Magnetism and Magnetic Materials 304, e312–e314 (2006).
15. Kopach, V., Kopach, O., Kanak, A., Shcherbak, L., Fochuk, P., Bolotnikov, A. E. and James, R. B., "Properties of $Cd_{0.90-x}Mn_xZn_{0.10}Te$ (x = 0.10, 0.20) crystals grown by Vertical Bridgman method," Proc. SPIE 10762, 1076212-1-8 (2018).